Calibration of numerical aperture effects in interferometric microscope objectives

Katherine Creath

The numerical aperture (N.A.) of a microscope objective can affect the measurement of surface profiles. Large N.A. objectives measure smaller heights than the actual values. An experiment to calibrate these effects on objectives with N.A.s of 0.1–0.95 is described using four traceable step height standards and a computer-controlled interferometric optical profiler utilizing phase-measurement interferometry techniques. The measured N.A. scaling factors have good agreement with a theory developed by Ingelstam. N.A. scaling factors are determined to an uncertainty of ± 1% for N.A.s ≤0.5 and ± 2% for N.A.s ≥0.9.

I. Introduction

It has been shown that the numerical aperture (N.A.) of an interferometric microscope objective can affect the fringe spacing and therefore the surface heights measured with that objective.[1] As the N.A. gets larger, the fringe spacing becomes larger, signifying that the distance between fringes will be greater than half a wavelength. This makes the measured surface heights smaller than they actually are. Because of this effect, a standard step will have more fringes across the step when measured with an N.A. = 0.1 than when measured with an N.A. = 0.95.

Many authors have tried to explain this phenomenon with theory.[2–5] However, most of their theories do not follow the published experimental measurements accurately. Other authors have discussed how different measurement geometries can affect these results. Their work indicates that the effective N.A. of the microscope objective as it is used to measure a particular sample, rather than the nominal N.A., will determine the effect on the fringe spacing.[5–7] Because most fringe analysis and phase-measurement algorithms assume that the surface heights change by simply half a wavelength per fringe, a calibration procedure is necessary to accurately determine height information.

This paper outlines an experiment using Michelson, Mirau, and Linnik interference microscope objectives along with a number of VLSI[8] step height standards to calibrate the change in fringe spacing or height with N.A.s ranging from 0.1–0.95. Measurements are obtained with the effective N.A. maximized by removing tilt fringes and centering the zero-order fringe in the field of view. A theory proposed by Ingelstam[5] yields the closest correspondence to the experimental data and can be used to determine the effective N.A.s of the microscope objectives tested.

II. Background

The N.A. of a microscope objective is defined as

$$\text{N.A.} = \sin\alpha_0, \tag{1}$$

where α_0 is half the total angle determined by the limiting aperture of the microscope objective illustrated in Fig. 1. As the N.A. becomes larger, the rays from larger incidence angles will get through the objective. Because of this, the fringe spacing increases, and fewer fringes are present. Since fewer fringes are present, a normal interpretation of the fringes having half a wavelength spacing would yield surface heights which are too small. This means that as the limiting cone angle of the objective increases, the actual height change from fringe to fringe increases and is greater than simply half a wavelength per fringe.

Various theories have been published to describe this phenomenon.[1–5] A paper by Tolmon and Wood started a series of papers discussing the effects of the obliquity angle on fringe spacing and height measurements using interferometric microscopes.[1] They published experimental data showing that the heights measured are smaller with high-power objectives than with low-power objectives. Gates then responded to this paper with a derivation of an N.A. factor which depends upon the limiting cone angle of the objective.[3] In this work, the fringe spacing is determined by inte-

The author is with WYKO Corporation, 1955 East Sixth Street, Tucson, Arizona 85719.

Received 17 March 1989.
0003-6935/89/163333-06$02.00/0.

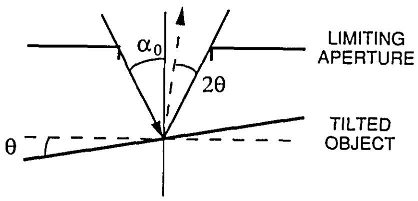

Fig. 1. Geometry showing maximum cone angle and effect of a tilted object on that angle.

grating over a circular aperture out to the maximum cone angle assuming a perfect optical system and weighting the aperture by the sine of the cone angle to weigh outer zones less than inner ones. The N.A. factor f determined by Gates is

$$f = \frac{\ln(\cos\alpha_0)}{\cos\alpha_0 - 1}, \tag{2}$$

where α_0 is the maximum cone angle given by the N.A. of the objective. The N.A. factor is always >1.0 and multiplies the surface heights to get a more accurate result. A simpler analysis was performed by Bruce and Thornton[4] in response to that of Gates finding an N.A. factor of

$$f = 1 + \frac{\alpha_0^2}{4}, \tag{3}$$

which assumes collimated light incident upon the objective and approximates $\cos\alpha_0$ with $1-0.5\alpha_0$. For large angles, this equation is not very accurate. However, it is better than that proposed by Gates. A paper which predates all of the previous work by Schulz[2] gives an expression for the N.A. factor of

$$f = \frac{2}{1 + \cos\alpha_0}, \tag{4}$$

which yields values in between those of Gates and Bruce and Thornton. The most accurate theory at high N.A.s is an equation derived by Ingelstam[5] which gives the N.A. factor as

$$f = 1 + \frac{\sin^2\alpha}{4} = 1 + \frac{(\text{N.A.}_{\text{eff}})^2}{4}, \tag{5}$$

where $\text{N.A.}_{\text{eff}} = \sin\alpha$ is the effective N.A., which is discussed in more detail below. Ingelstam assumes a partially spatially coherent source, a homogeneously illuminated circular entrance pupil, and a spectral coherence of the source much greater than the path difference. The intensity distribution of the interference fringes is found by integrating over the extended source.

In practice, the limiting aperture of the microscope is not necessarily equal to the nominal value listed on the objective. The tilt of the test surface, focal position of the test surface, local slope variations on the test surface, illumination, and coherence of the source can all affect this limiting cone angle. Because of this, the effective N.A. of the objective should be used to determine the performance of the system. However, the effective N.A. is difficult to determine theoretically. A few of the factors which influence the effective N.A. are illustrated below. The effective N.A. is best determined experimentally.

For a flat object tilted with respect to the reference surface which is assumed normal to the optical axis of the microscope, the effective N.A. can be easily written as[7]

$$\text{N.A.}_{\text{eff}} = \sin(\alpha_0 - \theta) = \sin\alpha, \tag{6}$$

where α_0 is the maximum cone angle of the objective, and θ is the tilt of the object surface (see Fig. 1). Note that this equation is 1-D. A more accurate theory needs to account for the change in area of the aperture.

The maximum tilt of the surface is limited by the depth of field of the objective. When the change in height of the surface equals the depth of field, the largest measurable tilt is determined by the arctangent of the depth of field divided by the profile length. The depth of field for a microscope objective is defined as[9]

$$\delta = \frac{\sqrt{1 - (\text{N.A.})^2}}{(\text{N.A.})^2}, \tag{7}$$

where λ is the wavelength of illumination. The profile length is given by the size of the image plane divided by the magnification. Using these definitions, the effective N.A.s for some typical microscope objectives with a 1-cm wide image plane are given in Table I. For N.A.s >0.25 the maximum tilt has a minimal impact on the effective N.A.

Other factors which can influence the effective N.A. are the focus position of the test surface relative to the reference surface, variations in the local slope of the test surface, the coherence of the source, and variations in illumination of the aperture. The focus position of the test surface relative to the reference surface, i.e., the position of the zero-order (equal path) fringe, affects the measurement by varying the cone angle with relative path length. The cone angle is larger on one side of focus than on the other side—thus changing the effective N.A. for different focus positions. It is assumed that focus is set for zero path difference so that the object and reference surfaces are both in focus. This effect is smaller than that caused by tilt when at the limits of the depth of field. Variations in the local slope of the object can also affect the effective N.A. Different field points will have different effective N.A.s. However, this should not be a large effect for most surfaces measured with an interferometric optical microscope. Additional discussions on determining effective N.A. can be found in the work of Ingelstam, Mycura and Rhead, and Dowell *et al.*[5–7]

Table I. Effective N.A.s for a Maximum Tilt of the Object Surface Limited by the Depth of Field with a 1-cm Wide Image Plane

Magnification	N.A.	Tilt angle (rad)	Effective N.A.
5	0.10	0.0323	0.068
10	0.25	0.0101	0.240
20	0.40	0.0074	0.393
40	0.50	0.0090	0.492
100	0.90	0.0035	0.898
200	0.95	0.0045	0.949

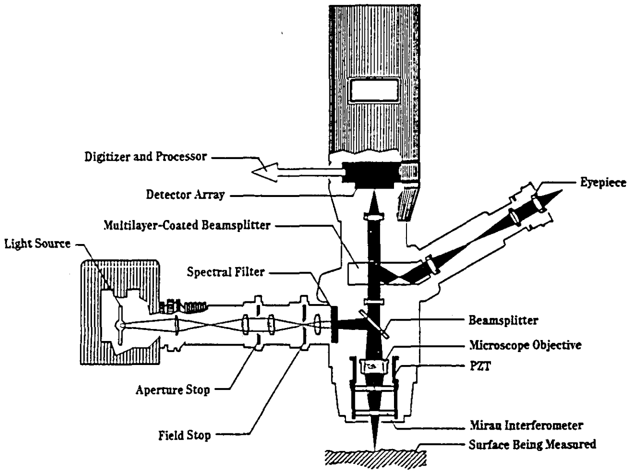

Fig. 2. Schematic of interferometric optical profiler.

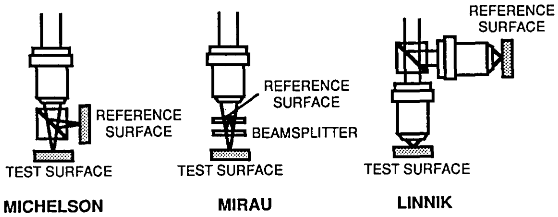

Fig. 3. Schematics of Michelson, Mirau, and Linnik interferometric microscope objectives.

As pointed out by Ingelstam, all of the theories for the N.A. factor should be written in terms of the effective N.A. When the surface under test is flat, smooth, positioned so that the fringes are fluffed out (less than one fringe of tilt), and the zero-order (darkest) fringe is in the field of view, then the effective N.A. is as close to the nominal value as possible. In this situation, the most accurate measurements can be made. Phase-measuring interferometry (PMI) techniques are ideal for this purpose because measurements can be made when the fringes are fluffed out.

III. Experiment

The instrument used in this work is the WYKO TOPO-3D. This instrument is a computer-controlled interferometric optical profiler using phase-measurement techniques to determine surface profiles. Its measurement principles have been explained in detail elsewhere.[10] A schematic of the system is shown in Fig. 2. Michelson, Mirau, and Linnik objectives are all used with this instrument (see Fig. 3). Low magnifications of 1.5×, 2.5×, and 5× use the Michelson interferometer. The middle magnifications 10×, 20×, and 40× use a Mirau interferometer, and high magnifications of 100× and 200× use a Linnik interferometer.

A piezoelectric transducer (PZT) moves the reference surface of the interferometer. Five frames of interferometric intensity data are taken at 90° relative phase increments of the path difference between the test and reference surfaces. Each of these frames can be written mathematically as

$$I_i(x,y) = I_0(x,y)\{1 + \gamma \cos[\phi(x,y) + \alpha_i]\}, \tag{8}$$

where $I_0(x,y)$ is the average intensity at each detector point, γ is the modulation of the fringe pattern, and α_i is the value of the relative phase shift between the object and reference beams for the ith exposure. These five frames of intensity are then combined point-by-point to determine the phase of the wavefront reflected from the test surface relative to the reference surface as imaged at the detector. The phase of the object's displacement $\phi(x,y)$ at the point (x,y) is given by

$$\phi(x,y) = \tan^{-1}\left\{\frac{2[I_2(x,y) - I_4(x,y)]}{2I_3(x,y) - I_5(x,y) - I_1(x,y)}\right\}, \tag{9}$$

where I_1, I_2, I_3, I_4, and I_5 are given by Eq. (8) with $\alpha_i = -\pi, -\pi/2, 0, \pi/2$, and π. Once the phase is determined, the surface heights are linearly related to the phase using

$$H(x,y) = \frac{f}{2}\left[\frac{\phi(x,y)\lambda}{2\pi}\right], \tag{10}$$

where λ is the wavelength of the source illumination, and f is N.A. factor. This technique enables the surface profiles to be measured directly without the need to interpret the interference fringes. It also can be used without placing tilt fringes within the field of view, so that the effective N.A. can be maximized.

The effect of the numerical aperture on step height measurements was determined experimentally by measuring four different VLSI step height standards which are traceable to NIST (The National Institute of Standards and Technology, formally The National Bureau of Standards, NBS). Each of these steps was measured using six different magnification objectives, each with a different N.A., on the computer-controlled interferometric optical profiler described above. A number of measurements were averaged for each objective, and multiple objectives at each magnification were used. The results for one magnification were averaged to determine the average step height for each N.A. At each location five separate measurements of the step were made without moving the step. Table II shows the objectives used, their magnification, N.A., the number of objectives measured, and the total number of measurements averaged to get the step height for each magnification.

The geometry of the VLSI steps and the measure-

Table II. Objectives Measured to Determine N.A. Factors Along with the Number of Measurements Averaged for Each Step Height

Objective magnification	N.A.	Num. obj. measured	Total meas. each step
5	0.10	1	5
10	0.25	5	25
20	0.40	6	30
40	0.50	4	20
100	0.90	1	40
200	0.95	2	80

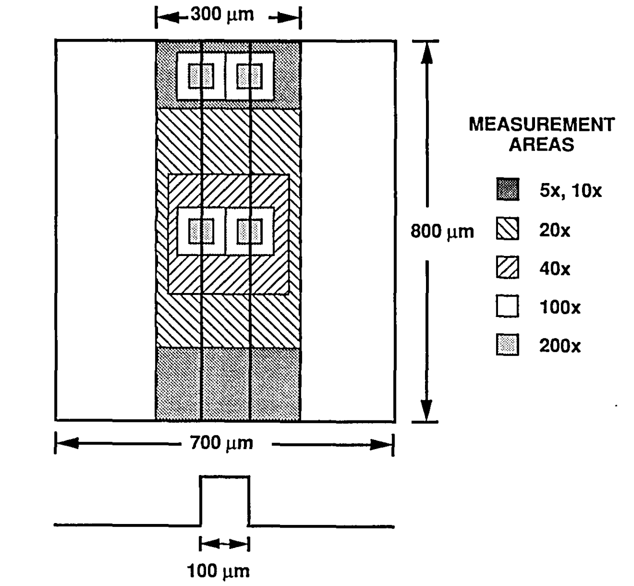

Fig. 4. Geometry of VLSI step standard showing step area and measurement area.

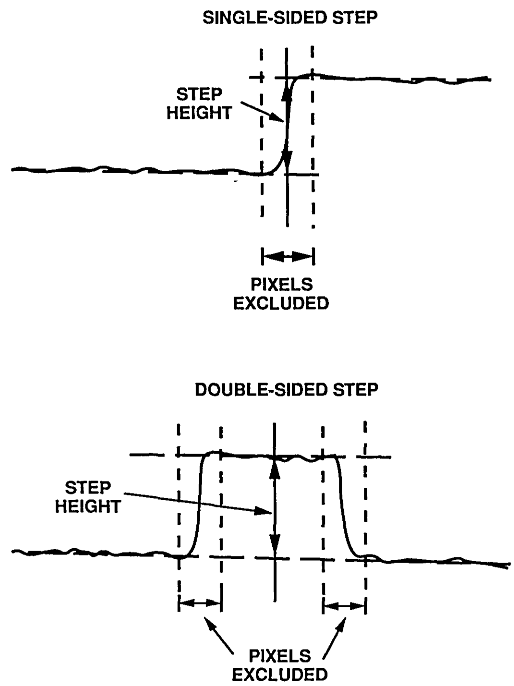

Fig. 5. Definitions for determination of step heights for single-sided and double-sided steps.

ment area over which the steps are measured are shown in Fig. 4. All steps are overcoated with chrome. The steps are raised relative to a substrate with an area of 100 μm wide × 800 μm long. The flat area around the step = 700 μm wide. The area measured = 300 μm wide centered on the step. For magnifications up to 10×, the entire step is measured. For 20×, the center 500 μm length is measured, for 40×, the center 250 μm, and for the 100× and 200× magnifications, four different locations are measured, each including only a single side of the step. Fields of view for each magnification are superimposed in Fig. 4.

VLSI certifies these steps by measuring them with a stylus. The scan length = 350 μm with five points sampled per μm. The step is measured in 10 different locations. These measurements are averaged with the highest and lowest thrown out. The step height is determined by averaging points at the top and the bottom of the step and taking that difference. The stylus is calibrated with a known step of the same height as being measured. The four steps used for this study are 43.5 nm ± 4.80%, 48.0 nm ± 4.76%, 83.4 nm ± 2.45%, and 85.5 nm ± 2.55%. These are the values quoted on the certificates provided by VLSI.

For this experiment, step heights are determined by first finding the step (largest discontinuity), and excluding the data in the immediate vicinity of the step. Lines are then fit in a least squares sense to the top and bottom of the steps. For a single-sided step, these lines are then extrapolated to the step discontinuity and the step height is the difference of these two lines at the discontinuity. For a double-sided step, lines are fit to the base and the top of the step and then the difference at the center of the step area is used as the step height. The step height is measured over many lines across a 3-D plot of the step and averaged to yield the step height. The limit to the number of lines averaged is the extent of the data, and the number of lines to average can be changed. Figure 5 shows the various parameters. The number of pixels excluded in the step region depends upon the field of view. For a large field of view, fewer points are discarded than for a small field of view. Discarding points in the step region ensures that the fit of the line does not include the rounded edges of the step.

For all measurements, each magnification head is calibrated and its repeatability measured to ensure that the system is functioning correctly. The darkest fringe (highest contrast) is always placed in the center of the field of view, and the reference surface is adjusted so that there is less than one fringe across the field of view. The tilt of the standard step is kept constant between measurements after being levelled. Two numbers, the step height and the standard deviation of the step heights for that measurement, are recorded. Five readings are taken for each step, only adjusting the focus to keep the darkest fringe in the center of the field of view. These readings are averaged to give an average step height for each step with each magnification head. Then the heights for each step height are averaged over all the different objectives used at one magnification.

IV. Results

A summary of the measurements is shown in Table III. Shown are the average step height using an N.A. factor of 1.0 to calculate the height for each magnification of 5× and greater, and the standard deviation of the step height values obtained with different objectives and operators. The N.A. factors for these raw data assuming that the stated VLSI step heights are correct are plotted in Fig. 6. The N.A. factors are found by dividing the stated height of the step by the measured height of the step. Note that the data all follow the same trend. The reason for the shifts in heights between the plots is due to inaccurate calibration of the step height standards. Assuming that the heights measured with the 5X objective are the correct heights (N.A. factor = 1.0 for 5X), and after shifting the data for each step so that they line up as well as possible to minimize the standard deviation at any objective, the data are replotted in Fig. 7, and the N.A. factors are shown in Table IV. Figure 7 also shows the average values shown in the table as the Average N.A. Factors. As can be seen from the data, the numerical aperture scaling factor has little effect for 40X objectives and below.

V. Comparison with Theory

The theories of Schulz, Gates, Bruce and Thornton, and Ingelstam have been used to tabulate the data shown in Table V for the objectives used in this experiment. The table shows the calculated N.A. factor for each objective using four different theories as well as the experimental values which have been adjusted by

Table III. Results of Step Height Measurements

Step height (nm)	Magnification	Measured step (nm)	Standard deviation (%)
43.50	5	39.35	—
	10	39.46	0.62
	20	39.11	1.29
	40	38.92	1.16
	100	33.49	3.50
	200	32.89	1.71
48.00	5	48.18	—
	10	48.10	0.72
	20	47.12	1.08
	40	47.08	0.78
	100	39.93	1.01
	200	39.44	1.08
83.40	5	83.63	—
	10	83.18	0.83
	20	81.46	0.64
	40	79.26	0.84
	100	68.00	0.59
	200	66.98	0.87
85.50	5	83.99	—
	10	83.07	0.79
	20	82.03	0.49
	40	80.95	0.96
	100	69.23	2.37
	200	69.67	3.24

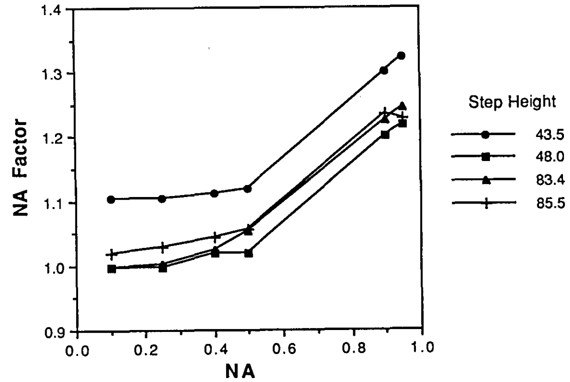

Fig. 6. Plot of raw data: N.A. factor plotted versus N.A. for four steps measured.

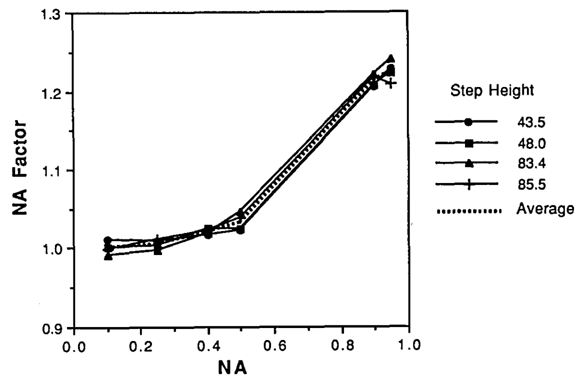

Fig. 7. Plots of N.A. factor versus N.A. after normalizing data to reduce the standard deviation of the N.A. factors at each magnification.

adding 0.003 to each value to correspond with the theoretical values at an N.A. of 0.1. For all of the numbers in the table below, the effective N.A. was assumed to be the entire N.A. This is true only if the surface is flat, the fringes are fluffed out, and the zero-order fringe is in the center of the field of view. Since the experimental results for the N.A. factors are lower than the theoretical results, it can be assumed that the objectives as used have a lower effective N.A. than that stated in the specifications. Figure 8 shows a plot of the different theories versus the experimental data.

At low N.A., all of the theories yield the same results. From the plot of Fig. 8, it is obvious that the equation by Ingelstam has the best agreement with the measured data at high N.A. This is in agreement with Dowell *et al.*[7] who show that Ingelstam's equation fits their data best. Dowell *et al.*[7] also show that the data

Table IV. Summary of N.A. factor results after shifting plots to line up on one another

Magnification	N.A.	N.A. factors 43.5	48.0	83.4	85.5	Average	Standard deviation
5	0.10	1.010	1.001	0.991	0.999	1.000	0.008
10	0.25	1.008	1.003	0.997	1.010	1.004	0.006
20	0.40	1.017	1.024	1.018	1.023	1.021	0.003
40	0.50	1.023	1.025	1.046	1.037	1.033	0.011
100	0.90	1.205	1.207	1.220	1.217	1.212	0.007
200	0.95	1.228	1.222	1.239	1.209	1.225	0.012

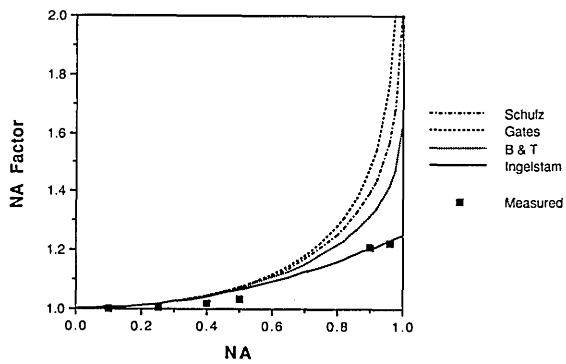

Fig. 8. Plot of N.A. factors versus N.A. to compare theory with measured values.

Table V. Comparison of Measured Data with Theory; the Measured Values Have Been Shifted by Adding 0.003 to Calculate Effective N.A.s

	N.A. factors					
N.A.	Schulz	Gates	Bruce and Thornton	Ingelstam	Measured (adjusted)	Effective N.A.
0.10	1.003	1.003	1.003	1.003	1.003	0.10
0.25	1.016	1.016	1.016	1.016	1.007	0.17
0.40	1.044	1.044	1.042	1.040	1.024	0.31
0.50	1.072	1.074	1.069	1.063	1.036	0.38
0.90	1.393	1.472	1.313	1.203	1.215	0.93
0.95	1.524	1.692	1.571	1.226	1.228	0.95

of Tolmon and Wood are fit best by the Ingelstam theory. Working backwards from the N.A. factors given by Ingelstam's theory, the effective N.A. for each objective in this experiment can be determined (see Table V). The effective N.A.s of the Linnik objectives are very close to the nominal values, but the Mirau objectives have a lower effective N.A. than expected. This is most likely due to the central obscuration caused by the reference surface.

VI. Conclusions

An experiment to measure the N.A. factors of microscope objectives with N.A.s ranging from 0.1–0.95 shows that at large N.A., scaling factors are necessary to give accurate height measurements. The N.A. factors can be determined by averaging many measurements using different step height standards and different objectives. For objectives of 40× magnification or less, or N.A.s ≤ 0.5, the N.A. factor has little effect on the measurement. However, at N.A.s ≥ 0.9, the measured heights are on the order of 20% too small, and the use of an N.A. scaling factor is essential to accurate measurements. The values of these N.A. scaling factors have an overall estimated uncertainty of ±1% for 10–40× and ±2% for 100–200×. The greatest contribution to the uncertainty in the N.A. factors is the quality of the VLSI step height standards.

When the experimental values are compared with theory, there is good agreement with a theory developed by Ingelstam. The effective N.A.s of the objectives calibrated in this work are very close to the nominal values because measurements were made with the test surface level with the reference surface (fringes fluffed out), and the zero-order fringe centered in the field of view, which is the best focus position. The Mirau objectives have a lower effective N.A. than the nominal value because of the central obscuration caused by the reference surface.

References

1. F. R. Tolmon and J. G. Wood, "Fringe Spacing in Interference Microscopes," J. Sci. Instrum. **33**, 236–238 (1956).
2. G. Schulz, "Uber Interferenzen Gleicher Dicke und Längenmessung mit Lichtwellen," Ann. Phys. **14**, 177–187 (1954).
3. J. W. Gates, "Fringe Spacing in Interference Microscopes," J. Sci. Instrum. **33**, 507–507 (1956).
4. C. F. Bruce and B. S. Thornton, "Obliquity Effects in Interference Microscopes," J. Sci. Instrum. **34**, 203–204 (1957).
5. E. Ingelstam, "Problems Related to the Accurate Interpretation of Microinterferograms," in *Interferometry*, National Physical Laboratory Symposium No. 11 (Her Majesty's Stationery Office, London, 1960), pp. 141–163.
6. H. Mykura and G. E. Rhead, "Errors in Surface Topography Measurements with High Aperture Interference Microscopies," J. Sci. Instrum. **40**, 313–315 (1963).
7. M. B. Dowell, C. A. Hultman, and G. M. Rosenblatt, "Determination of Slopes of Microscopic Surface Features by Nomarski Polarization Interferometry," Rev. Sci. Instrum. **48**, 1491–1497 (1977).
8. Standards manufactured by VLSI Standards, Inc., 2660 Marine Way, Mountain Valley, CA 94043.
9. J. R. Benford, "Microscope Objectives," in *Applied Optics and Optical Engineering, Vol. 3*, R. Kingslake, Ed. (Academic, New York, 1966), pp. 145–182.
10. J. C. Wyant, C. L. Koliopoulos, B. Bhushan, and D. Basila, "Development of a Three-dimensional Noncontact Digital Optical Profiler," Trans. ASME J. Tribology **108**, 1–8 (1986).